Effects of elastic strain and structural defects on slow light modes in a one-dimensional array of microcavities

Article *in* Superlattices and Microstructures · June 2018
DOI: 10.1016/j.spmi.2018.06.043

5 authors, including:

Vladimir Rumyantsev
National Academy of Sciences of Ukraine
106 PUBLICATIONS **102** CITATIONS
SEE PROFILE

Alexey Kavokin
University of Southampton
54 PUBLICATIONS **58** CITATIONS
SEE PROFILE

Superlattices and Microstructures 120 (2018) 642–649

Contents lists available at ScienceDirect

Superlattices and Microstructures

journal homepage: www.elsevier.com/locate/superlattices

Effects of elastic strain and structural defects on slow light modes in a one-dimensional array of microcavities

Vladimir Rumyantsev[a,b], Stanislav Fedorov[a], Kostyantyn Gumennyk[a,*], Denis Gurov[a], Alexey Kavokin[b,c,d,e]

[a] Galkin Institute for Physics & Engineering, Donetsk, 83114, Ukraine
[b] Mediterranean Institute of Fundamental Physics, 00047, Marino, Rome, Italy
[c] Physics and Astronomy School, University of Southampton, Highfield, Southampton, SO171BJ, United Kingdom
[d] CNR-SPIN, Viale del Politecnico 1, I-00133, Rome, Italy
[e] Spin Optics Laboratory, St. Petersburg State University, St. Petersburg, 198504, Russia

ARTICLE INFO

Keywords:
Microcavity
Quantum dot
Polariton
Photonic crystal

ABSTRACT

We calculate the dispersion of exciton-polariton modes in one-dimensional arrays of microcavities. We consider a two-sublattice array and a one-sublattice array of unevenly spaced spherical microcavities some of which contain embedded quantum dots. In both cases the dispersion of polariton eigen modes is shown to be efficiently controlled by a weak applied uniform strain. The structures we consider sustain slow-light modes that are of a specific importance for quantum optics applications. The high sensitivity of the optical response of microcavity arrays to the applied strain may be used in classical and quantum optical switches and the polariton based integrated photonics.

1. Introduction

The design of sources of coherent radiation based on new structures and materials is an extensive interdisciplinary research area that combines the laser physics, condensed matter physics, nanotechnology, chemistry, and information science. One of the important challenges in this field is controlling the propagation of light in resulting composite structures by subjecting them to various kinds of external actions such as e.g. elastic strains [1]. From this point of view, photonic superstructures based on optical microcavities with embedded non-linear elements (e.g. semiconductor quantum dots) represent one of the most promising systems for integration in future optical circuits [2,3]. Arrays of coupled optical cavities as well as periodic arrays of coupled exciton/cavities have been considered in Refs. [4,5].

In this context, a rapidly developing research sub-area is the photonics of imperfect structures. Some of our previous works have been devoted to the design of multi-microcavity structures [6] where the dispersion of photon modes may be altered by introduction of a defect in the photonic supercrystal [7,8]. For applications, the structural defects in supercrystals are less practical than temporary defects introduced by application of external fields or strain.

In the present work we consider the effect of a uniform elastic strain (which is assumed to be much weaker than any breaking deformation) on one-dimensional arrays of microcavities with embedded quantum dots. This system combines advantages of an extreme optical non-linearity provided by the coupling of quantum dots to photonic modes and the high sensitivity of the optical eigen-modes to the applied strain. We focus on two particular realizations of a topologically ordered microcavity system composed by

* Corresponding author.
E-mail address: kgumennyk@gmail.com (K. Gumennyk).

https://doi.org/10.1016/j.spmi.2018.06.043
Received 7 May 2018; Received in revised form 21 June 2018; Accepted 21 June 2018
Available online 21 June 2018

tunnel-coupled optical microcavities: a two-sublattice array and a one-sublattice array of unevenly spaced spherical microcavities. We show that both systems have a high potentiality for applications in optical integrated circuits.

2. Theoretical background

Basing on the approach developed in Refs. [7–10], let us first consider the dispersion of optical eigen modes in the most general case of a microcavity supercrystal composed of s sublattices. Each of the tunnel-coupled microcavities is assumed to confine a single optical mode. In the considered cases of elastic deformations in chains of microcavities with embedded quantum dots and otherwise, Hamiltonian $\hat{H}(\hat{\varepsilon})$ depends on the deformation tensor $\hat{\varepsilon}$, which is a function of the applied strain. Under the assumption that the density of excited states of structural elements in the resonator and atomic subsystems is a small quantity, the quadratic part $\hat{H}^{ex}(\hat{\varepsilon})$ (responsible for the elementary excitations) of Hamiltonian $\hat{H}(\hat{\varepsilon})$ within the Heitler-London approximation and a one-level model can be written as (see e.g. Ref. [11]):

$$\hat{H}^{ex}(\hat{\varepsilon}) = \sum_{\mathbf{n},\mathbf{m},\alpha,\beta,\lambda,\sigma} D^{\lambda\sigma}_{\mathbf{n}\alpha,\mathbf{m}\beta}(\hat{\varepsilon})\hat{\Phi}^{+}_{\mathbf{n}\alpha\lambda}\hat{\Phi}_{\mathbf{m}\beta\sigma} = \sum_{\alpha,\beta,\lambda,\sigma,\mathbf{k}} D^{\lambda\sigma}_{\alpha\beta}(\mathbf{k},\hat{\varepsilon})\hat{\Phi}^{+}_{\alpha\lambda}(\mathbf{k})\hat{\Phi}_{\beta\sigma}(\mathbf{k}), \tag{1}$$

where

$$D^{11}_{\mathbf{n}\alpha,\mathbf{m}\beta}(\hat{\varepsilon}) = \hbar\omega^{at}_{\mathbf{n}\alpha}\delta_{\mathbf{n}\alpha,\mathbf{m}\beta} + V_{\mathbf{n}\alpha,\mathbf{m}\beta}(\hat{\varepsilon}),\quad D^{22}_{\mathbf{n}\alpha,\mathbf{m}\beta} = \hbar\omega^{ph}_{\mathbf{n}\alpha}\delta_{\mathbf{n}\alpha,\mathbf{m}\beta} - A_{\mathbf{n}\alpha,\mathbf{m}\beta}(\hat{\varepsilon}),\quad D^{12}_{\mathbf{n}\alpha,\mathbf{m}\beta}(\hat{\varepsilon}) = D^{21}_{\mathbf{n}\alpha,\mathbf{m}\beta}(\hat{\varepsilon}) = g_{\mathbf{n}\alpha}(\hat{\varepsilon})\delta_{\mathbf{n}\alpha,\mathbf{m}\beta},\quad \hat{\Phi}^{\lambda=2}_{\mathbf{n}\alpha} = \hat{\Psi}_{\mathbf{n}\alpha},\quad \hat{\Phi}^{\lambda=1}_{\mathbf{n}\alpha} = \hat{B}_{\mathbf{n}\alpha}. \tag{2}$$

In Eqs. (1) and (2) $\omega^{ph}_{\mathbf{n}\alpha}$ is the frequency of the photonic mode localized in the $\mathbf{n}\alpha$-th lattice site (microcavity), $\hat{\Psi}^{+}_{\mathbf{n}\alpha}$, $\hat{\Psi}_{\mathbf{n}\alpha}$ are bosonic creation and annihilation operators for this mode written in the node representation, $\hbar\omega^{at}_{\mathbf{n}\alpha}$ is excitation energy of the quantum dot in the $\mathbf{n}\alpha$-th lattice site, $\hat{B}_{\mathbf{n}\alpha}$, $\hat{B}^{+}_{\mathbf{n}\alpha}$ are bosonic creation and annihilation operators of quantum dot excitons, $A_{\mathbf{n}\alpha\mathbf{m}\beta}(\hat{\varepsilon})$ is the matrix of resonance interaction, which describes an overlap between optical fields of resonators in the $\mathbf{n}\alpha$-th and $\mathbf{m}\beta$-th lattice sites and hence defines the jump probability of the corresponding electromagnetic excitation, $V_{\mathbf{n}\alpha\mathbf{m}\beta}(\hat{\varepsilon})$ is the matrix of resonance interaction between quantum dots embedded in the $\mathbf{n}\alpha$-th and $\mathbf{m}\beta$-th lattice sites, $g_{\mathbf{n}\alpha}(\hat{\varepsilon})$ is the matrix of resonance interaction between quantum dot in the $\mathbf{n}\alpha$-th lattice site and electromagnetic field localized at the same site. Values 1 and 2 of indices λ, σ indicate, respectively, the presence or absence of quantum dots in corresponding cavities.

In the right-hand side expression of Eq. (1) (summation over $\mathbf{k}$) matrices $D^{\lambda\sigma}_{\alpha\beta}(\mathbf{k},\hat{\varepsilon})$ and $\Phi_{\alpha\lambda}(\mathbf{k})$ have the forms $D^{\lambda\sigma}_{\alpha\beta}(\mathbf{k},\hat{\varepsilon}) = \sum_{\mathbf{m}} D^{\lambda\sigma}_{\mathbf{n}\alpha\mathbf{m}\beta}(\hat{\varepsilon})\exp[i\mathbf{k}\cdot(\mathbf{r}_{\mathbf{n}\alpha} - \mathbf{r}_{\mathbf{m}\beta})]$ and $\hat{\Phi}_{\alpha\lambda}(\mathbf{k}) = \frac{1}{\sqrt{N}}\sum_{\mathbf{n}}\hat{\Phi}_{\mathbf{n}\alpha\lambda}\exp(-i\mathbf{k}\cdot\mathbf{r}_{\mathbf{n}\alpha})$ (N is the number of elementary cells in the lattice). Such representation of matrices is possible due to preservation of the translation invariance of the system under the uniform strain. Let us note that the wave vector $\mathbf{k}$, which characterizes eigenstates of electromagnetic excitations, ranges within the first supercrystal Brillouin zone, whose boundaries are in their turn functions of strain through the dielectric tensor $\hat{\varepsilon}$.

Eigenvalues of the Hamiltonian (1) are found by its diagonalization through the Bogolyubov-Tyablikov transformation [11]. This yields the following equation for elementary excitation spectrum $\Omega(\mathbf{k},\hat{\varepsilon})$:

$$\det\|D^{\lambda\sigma}_{\alpha\beta}(\mathbf{k},\hat{\varepsilon}) - \hbar\Omega(\mathbf{k},\hat{\varepsilon})\delta_{\alpha\beta}\delta_{\lambda\sigma}\| = 0 \tag{3}$$

On the basis of this equation below we investigate in detail the spectrum of exciton-polariton modes in a two-sublattice chain of microcavities and in a one-sublattice chain of unevenly spaced cavities with embedded quantum dots.

3. Results and discussion

3.1. Exciton-like excitations in a one-dimensional two-sublattice microcavity array under a uniform elastic strain

Let us consider a one-dimensional microcavity chain subjected to the elastic strain (extension or compression) directed along the chain. Under a uniform strain described by the dielectric tensor $\hat{\varepsilon}$ each cavity changes its position so that the lattice constant $d(\varepsilon)$ varies as:

$$d(\varepsilon) = (1+\varepsilon)d_0, \tag{4}$$

where d_0 is the lattice constant of a strain-free structure, and ε is the corresponding component of tensor $\hat{\varepsilon}$. The reciprocal lattice constant $b(\varepsilon)$ can be obtained from the simple relation:

$$b(\varepsilon)\cdot d(\varepsilon) = 2\pi, \tag{5}$$

In what follows we shall assume that the microcavity array is constituted by two sublattices. Positions of microcavities are defined by the equality $r_{n\alpha}(\varepsilon) = r_n(\varepsilon) + r_\alpha(\varepsilon)$. For example, the positions in the zeroth cell of the first and second sublattices ($r_{n=0} = 0$) are given by: $r_{01} = 0$ and $r_{02}(\varepsilon) = a(\varepsilon)$, respectively. The spectrum of exciton-like excitations $\Omega(k,\varepsilon)$ is found from the relation (3) as:

$$\begin{Vmatrix} \hbar\Omega(k,\varepsilon) - \hbar\omega^{ph}_1(\varepsilon) & A_{12}(k,\varepsilon) \\ A_{21}(k,\varepsilon) & \hbar\Omega(k,\varepsilon) - \hbar\omega^{ph}_2(\varepsilon) \end{Vmatrix} = 0 \tag{6}$$

The quantities $A_{\alpha\beta}(k,\varepsilon)$ in Eq. (6) are the Fourier-transforms of matrix $A_{n\alpha m\beta}(\varepsilon)$ of resonance interaction:

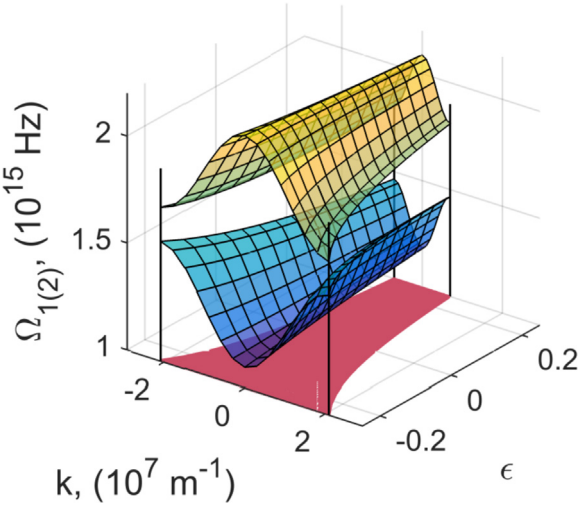

Fig. 1. Dispersion surfaces $\Omega_{1(2)}(k, \varepsilon)$ of the two-sublattice microcavity array subjected to a uniform elastic strain.

$A_{\alpha\beta}(k, \varepsilon) = \sum_m A_{n\alpha m\beta}(\varepsilon)\exp\{ik[r_{n\alpha}(\varepsilon) - r_{m\beta}(\varepsilon)]\}$. In the framework of our model and within the nearest-neighbor approximation the matrix elements $A_{\alpha\beta}(k, \varepsilon)$ can be represented as follows:

$$A_{12}(k, \varepsilon) \cong A_{12}[a(\varepsilon)]\exp[-ik{\cdot}a(\varepsilon)] + A_{12}[d(\varepsilon) - a(\varepsilon)]\exp\{-ik{\cdot}[d(\varepsilon) - a(\varepsilon)]\},$$
$$A_{21}(k, \hat{\varepsilon}) = A_{21}[a(\varepsilon)]\exp[ik{\cdot}a(\varepsilon)] + A_{21}[d(\varepsilon) - a(\varepsilon)]\exp\{ik{\cdot}[d(\varepsilon) - a(\varepsilon)]\}\ , \quad (7)$$

According to Ref. [12], quantities $A_{12(21)}[a(\varepsilon)]$, which are components of matrix $A_{n\alpha m\beta}(\varepsilon)$ of resonance interaction, corresponding to nearest neighbors, equal to $A_{12(21)}[a(\varepsilon)] = A_{12(21)}(a)\exp(-\varepsilon)$, $A_{12(21)}[d(\varepsilon) - a(\varepsilon)] = A_{12(21)}(d - a)exp(-\varepsilon)$. In our case we put $A_{12}(a) \simeq A_{21}(a)$, $A_{12}(d - a) \simeq A_{21}(d - a)$. The relation (6) shows that the dispersion $\Omega(k, \varepsilon)$ of elementary electromagnetic excitations is governed both by frequency characteristics of the microcavity array and by the explicit form of $A(k, \varepsilon)$, as well as by the sign of strain (i.e. if a uniaxial extension $\varepsilon > 0$ or contraction $\varepsilon < 0$ is applied).

Further calculations were performed for the case of a uniaxial strain of a uniform isotropic one-dimensional medium. The following modeling parameters were adopted: frequencies of resonance photonic modes in cavities (independent of deformation ε) were taken as $\omega_1^{ph} = 2\pi \times 211THz$ and $\omega_2^{ph} = 2\pi \times 310THz$. The other parameters of our calculation are as follows: $A_{12}(a)/2\hbar = 0.9{\cdot}10^{14}Hz$, $A_{12}(d - a)/2\hbar = 1.2{\cdot}10^{14}Hz$, $a = 1{\cdot}10^{-7}m$, $d = 9{\cdot}10^{-7}m$. Fig. 1 shows surfaces $\Omega_\nu(k, \varepsilon)$, $(\nu = 1,2)$ calculated for the strained one-dimensional lattice for various values of ε. The shaded region in the (k, ε)-plane corresponds to the first Brillouin zone.

An important property of band gap photonic structures is their ability to sustain the so-called “slow light”. It has important application in designing quantum optical information processing devices. The effective decrease of quasiparticle group velocity was shown to occur in coupled wave-guide optical cavities [13] and in various types of multilayer semiconductor structures [14]. The reduction of the group velocity is caused by relatively heavy effective masses of photons and exciton-polaritons in the considered

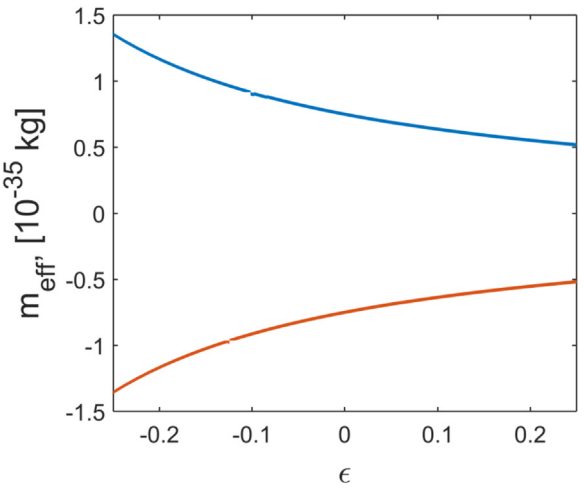

Fig. 2. Dependences of the effective masses of the propagating photonic modes in on the applied strain in a two-sublattice microcavity array.

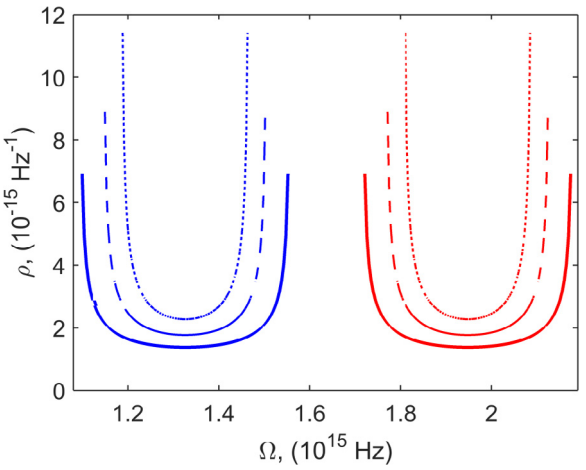

Fig. 3. Strain-induced changes of the density of polaritonic states $\rho_{\pm}(\Omega, \varepsilon)$ in the lower and upper dispersion bands in a two-sublattice microcavity array. Dotted curves correspond to $\varepsilon = -0.25$; dashed curves correspond to $\varepsilon = 0$; solid curves correspond to $\varepsilon = 0.25$.

microcavity supercrystals, $m_{eff\,(\nu)}$ $(\nu = 1;\ 2)$ Fig. 2 shows the dependence of the effective mass $m_{eff\,(\nu)} = \hbar\left[\frac{\partial^2\Omega_\nu(k,\varepsilon)}{\partial k^2}\Big|_{k=0}\right]^{-1}$ of the considered exciton-like excitations on the applied strain. It follows from this graph that an changing ε one can efficiently control the group velocity of the slow light mode.

It is often important to know how the peculiarities of the spectrum are manifested in the quasiparticles density of states $\rho_\nu(\Omega, \varepsilon)$, which obviously should also depend on the strain. According to Ref. [15] in our case the functions $\rho_\nu(\Omega, \varepsilon)$ are given by:

$$\rho_\nu(\Omega, \hat{\varepsilon}) = \frac{d(\varepsilon)}{2\pi}\sum_i \frac{1}{\left|\frac{d\Omega_\nu(\varepsilon,k)}{dk}\right|_{k_i}}, \tag{8}$$

where k_i are the roots of equation $\Omega_\nu(k) = \Omega$. Calculation in (8) is carried out for the values of wave vector k falling within the first Brillouin zone. Densities of states $\rho_\nu(\Omega)$ of quasiparticles in upper and lower dispersion branches are plotted in Fig. 3 for several values of ε.

3.2. Polaritons in a one-sublattice quantum-dot-containing chain of unevenly spaced microcavities under a uniform elastic deformation

In this section we shall consider a more complex system of a one-sublattice array of identical cavities with randomly embedded quantum dots of two types, whose concentrations are, correspondingly, $C_C^{(1)}$ and $C_C^{(2)}$. It is assumed, in addition, that microcavities are unevenly spaced; namely that $C_T^{(1)}$ neighboring pairs of cavities are separated by distance $a_1(\varepsilon)$ and the remaining $C_T^{(2)}$ pairs are separated by distance $a_2(\varepsilon)$. Here we also adopt the virtual crystal approximation [16,17] based on the diagonalization of the averaged Hamiltonian (1). The corresponding procedure yields a system of uniform linear equations, whose solvability condition is given by:

$$\begin{Vmatrix} \hbar\langle\omega_n^{at}(\varepsilon)\rangle_C + \langle V(k,\varepsilon)\rangle_{C,T} - \hbar\Omega(k,\varepsilon) & \langle g_n(\varepsilon)\rangle_C \\ \langle g_n(\varepsilon)\rangle_C & \hbar\omega^{ph}(\varepsilon) - \langle A(k,\varepsilon)\rangle_T - \hbar\Omega(k,\varepsilon) \end{Vmatrix} = 0, \tag{9}$$

where $\langle\omega_n^{at}\rangle_C = \sum_{\nu=1}^2 \omega_\nu^{at} C_C^\nu$, $\langle g_n\rangle_C = g^{(1)}C_C^{(1)} + g^{(2)}C_C^{(2)}$, (it is implied that $C_C^{(1)} + C_C^{(2)} = 1$, and hence $C_C^{(1)} = 1 - C_C^{(2)} \equiv C_C$); $\langle V(k)\rangle_{C,T} = \sum_{\nu,\mu=1}^2 V^{\nu\mu}(k,\{C_T\},\varepsilon)C_C^\nu C_C^\mu$, $V^{\nu,\mu}(k,\{C_T\},\varepsilon) = \sum_m \langle V_{nm}^{\nu\mu}(\varepsilon)\rangle_T \exp[ikr_{nm}(\{C_T\},\varepsilon)]$. Similarly, $A(k,\{C_T\},\varepsilon) = \sum_m \langle A_{nm}(\varepsilon)\rangle_T \exp[ikr_{nm}(\{C_T\},\varepsilon)]$,where $r_{nm}(\{C_T\},\varepsilon) = d(\{C_T\},\varepsilon)(n-m)$, $(C_T^{(1)} + C_T^{(2)} = 1,\ C_T^{(1)} = 1 - C_T^{(2)} \equiv C_T)$.

Angular brackets in (9) denote the procedure of configuration averaging of the microcavity array over all possible positions of cavities (index "T") and compositions of quantum dots (index "C"). $d(\{C_T\},\varepsilon)$ is the period of the "virtual" one-dimensional microcavity lattice obtained by averaging $d(\{C_T\},\varepsilon) = C_T^{(1)}a_1(\varepsilon) + C_T^{(2)}a_2(\varepsilon)$.

Within the nearest-neighbor approximation, the quantities $V(k,\{C_T\},\varepsilon)$, $A(k,\{C_T\},\varepsilon)$ can be found as:

$$\begin{bmatrix} V^{\nu\mu}(k,\{C_T\},\varepsilon) \\ A^{\nu\mu}(k,\{C_T\},\varepsilon) \end{bmatrix} = 2\begin{bmatrix} V^{\nu\mu}[d(\{C_T\},\varepsilon),\varepsilon] \\ A^{\nu\mu}[d(\{C_T\},\varepsilon),\varepsilon] \end{bmatrix}\cos\{kd[\{C_T\},\varepsilon]\} \tag{10}$$

It follows from (9) that the dispersion relation $\Omega(k,\{C_C, C_T\},\varepsilon)$ of polariton modes is defined by frequency characteristics of the cavities and the dots as well as by the explicit form of expressions $A(k,\{C_T\},\varepsilon)$ and $V^{\nu,\mu}(k,\{C_T\},\varepsilon)$. In the framework of our model, the functions $A[d(\{C_T\},\varepsilon),\varepsilon]$ and $V^{\nu\mu}[d(\{C_T\},\varepsilon),\varepsilon]$ of the strain degree and the defect concentrations are assumed (for $a_2(\varepsilon) > a_1(\varepsilon)$) to be equal to:

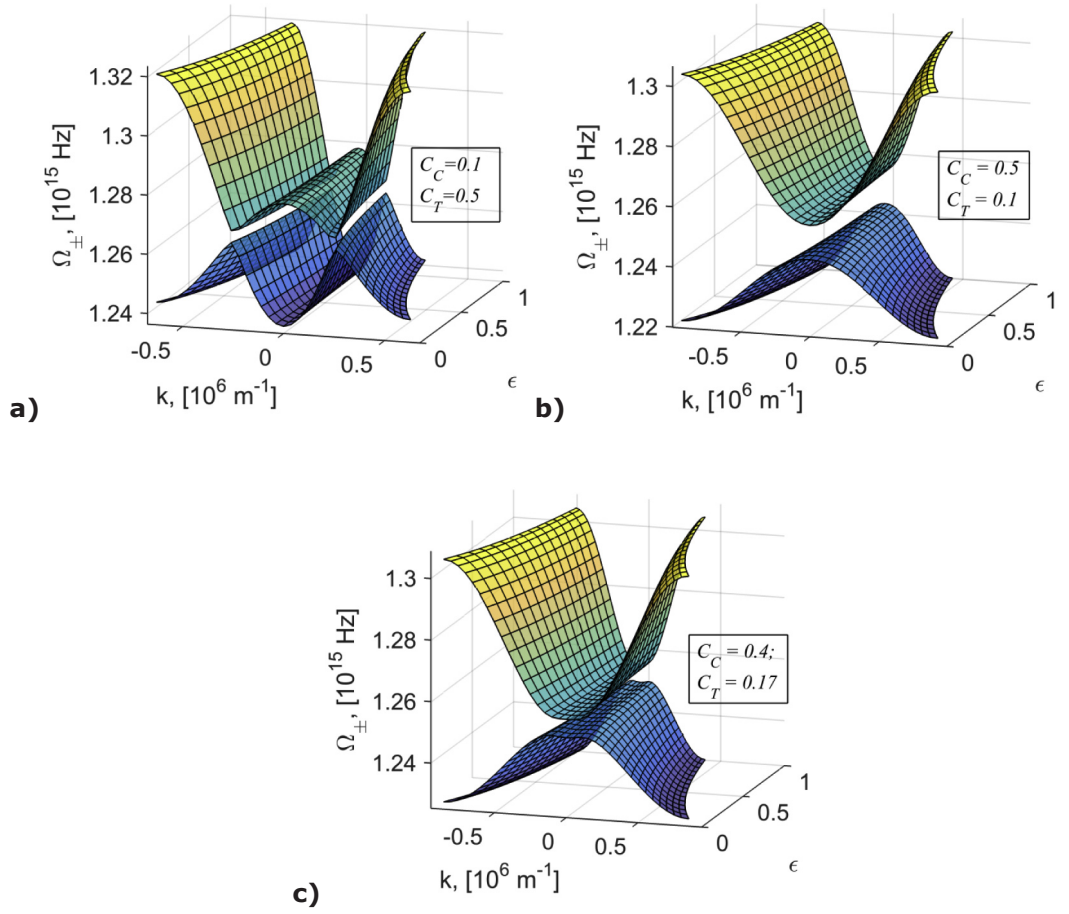

Fig. 4. Dispersions $\Omega_{\pm}(k, C_C, C_T)$ of polaritonic excitations in a one-sublattice quantum-dot-containing chain of unevenly spaced microcavities plotted for different values of the dot concentrations C_C, C_T. Fig. 4c has been plotted for the values of concentrations corresponding to the black asterisk in Fig. 7 and it demonstrates the case of both effective polaritonic masses $m_{eff}^{(\pm)}$ being positive.

$$\begin{bmatrix} V^{\nu\mu}[d(\{C_T\}, \varepsilon), \varepsilon] \\ A[d(\{C_T\}, \varepsilon), \varepsilon] \end{bmatrix} = \begin{bmatrix} V^{\nu\mu}(a_1|_{\varepsilon=0}) \\ A(a_1|_{\varepsilon=0}) \end{bmatrix} \exp\left[-\frac{|d(\{C_T\}, \varepsilon) - a_1(\varepsilon)|}{a_1(\varepsilon)} - \varepsilon \right], \tag{11}$$

$a_1|_{\varepsilon=0} \equiv a_1$, $a_2|_{\varepsilon=0} \equiv a_2$. Quantities $A(a_1)$, $V^{\nu\mu}(a_1)$ characterize an overlap of optical fields of neighboring cavities and an interaction between neighboring quantum dots in a one-dimensional lattice with period a_1, respectively. Such a lattice is chosen to be a reference one for the subsequent variation of distances between resonators.

Similarly to our previous works [6–8], the numerical calculations were carried out for the following modeling values of parameters corresponding to real resonator systems (see e.g. Refs. [9,18]) and leading to polariton effect. The frequency of cavity-localized resonance photonic modes was put equal to $\omega^{ph} = 2\pi \times 203\ THz \approx 1280{\cdot}10^{12} Hz$; the two types of quantum dots were assumed to be characterized by the exciton resonance frequencies $\omega_1^{at} = 2\pi{\cdot}191\ THz \approx 1200{\cdot}10^{12}\ Hz$ and $\omega_2^{at} = 2\pi{\cdot}202\ THz \approx 1269{\cdot}10^{12}\ Hz$, whereas $A/2\hbar = 8{\cdot}10^{13} Hz$, $V^{11}/2\hbar = 1\ {\cdot}10^{13} Hz$, $V^{22}/\hbar = 3\ {\cdot}10^{13} Hz$, $V^{12} \approx V^{21} = 6{\cdot}10^{13} Hz$, $g^{(1)}/\hbar = 5{\cdot}10^{12}\ Hz$, $g^{(2)}/\hbar = 1.5{\cdot}10^{12}\ Hz$ (within the adopted approximation the magnitude of resonance interaction of a quantum dot with an electromagnetic field localized at the same cavity is independent of deformation ε). The lattice periods were set equal to $a_1 = 3{\cdot}10^{-6} m$ and $a_2 = 7{\cdot}10^{-6} m$. The two dispersion branches $\Omega_{\pm}(k, C_C, C_T)$ of the considered collective excitations in the microcavity array are plotted in Figs. 4a–c for several values of C_C and C_T. It should be noted that the shape of the dispersion curve in Fig. 4a indicates the existence of Bose-Einstein exciton condensate, where the energy minima occur for a number of states with non-zero k's (in addition to those with $k = 0$). Let us remind that k ranges between $-\frac{\pi}{a_2(\varepsilon) + C_T[a_1(\varepsilon) - a_2(\varepsilon)]} \le k \le +\frac{\pi}{a_2(\varepsilon) + C_T[a_1(\varepsilon) - a_2(\varepsilon)]}$, whereas C_T ranges between 0 and 1. The concentration dependence of the band gap width $\Delta\Omega(\varepsilon, k, C_C, C_T) \equiv \min_k[\Omega_+(\varepsilon, k, C_C, C_T) - \Omega_-(\varepsilon, k, C_C, C_T)]$ is shown in Fig. 5. The non-monotonous character of concentration dependence $\Omega_{\pm}(\varepsilon, k, C_C, C_T)$ reflects the specifics of disorderliness of the system and is manifested in the character of effective masses of quasiparticles $m_{eff}^{(\pm)}(\varepsilon, C_C, C_T) \equiv \hbar\left(\frac{\partial^2\Omega_{\pm}(\varepsilon, k, C_C, C_T)}{\partial k^2}\Big|_{k=0}\right)^{-1}$ (Figs. 6a–d, 7).

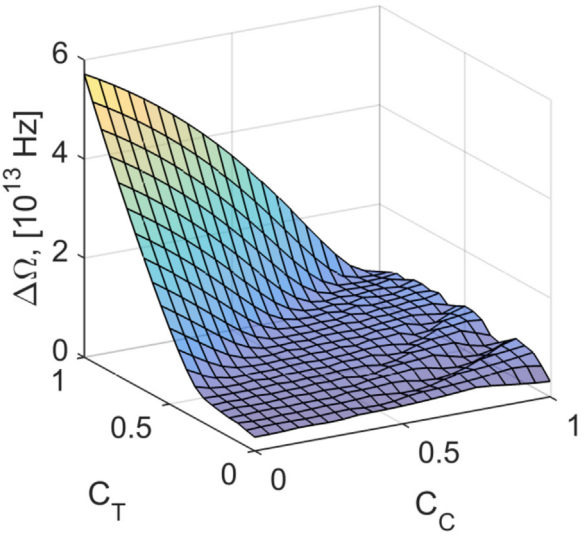

Fig. 5. Polaritonic band gap in a one-sublattice quantum-dot-containing chain of unevenly spaced microcavities plotted as a function of concentrations of quantum dots C_C, C_T.

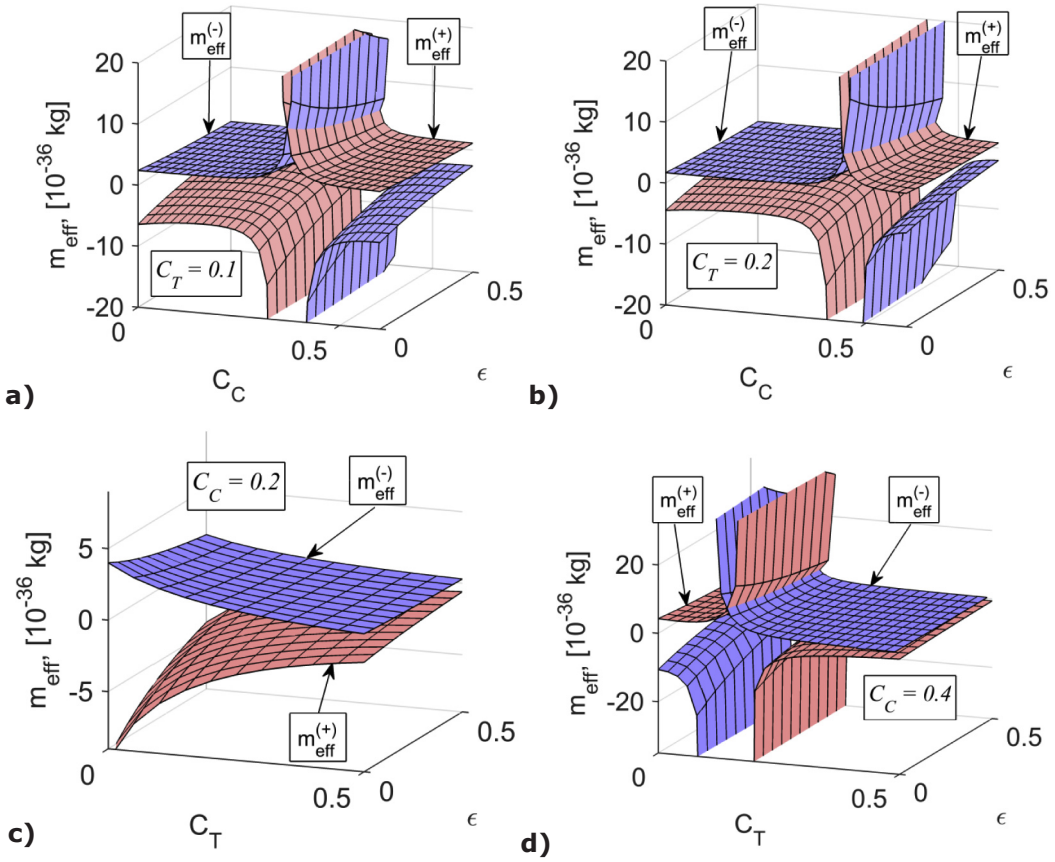

Fig. 6. Effective masses of polaritons in a one-sublattice quantum-dot-containing chain of unevenly spaced microcavities as functions of the quantum dot concentrations C_C, C_T. and the strain. Calculations in Fig. 6a–d have been performed along the lines in the C_C–C_T. -plane shown in Fig. 7.

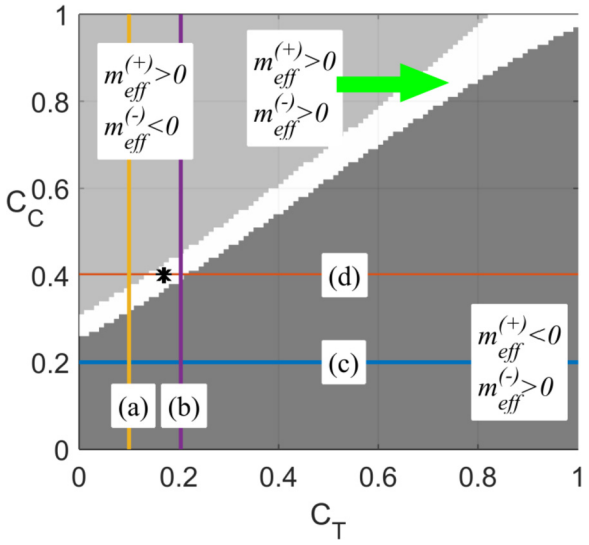

Fig. 7. The sign of effective masses $m_{eff}^{(\pm)}$ of polaritons in a one-sublattice quantum-dot-containing chain of unevenly spaced microcavities for different concentrations of quantum dots in the photonic supercrystal. The edges of shaded areas correspond to singularities of effective masses $m_{eff}^{(\pm)}$ (see Figs. a, b and d).

These results are completed by calculations of the density of states of corresponding quasiparticles $\rho(\Omega, \varepsilon, C_C, C_T)$. In the present case, the function $\rho(\Omega, \varepsilon, C_C, C_T)$ has the form:

$$\rho_\nu(\Omega, \hat{\varepsilon}, C_C, C_T) = \frac{d(\varepsilon, C_T)}{2\pi} \sum_i \frac{1}{\left|\frac{d\Omega_\nu(\varepsilon, k, C_C, C_T)}{dk}\right|_{k_i}} \tag{12}$$

Summation in (12) is carried out over various values of the wave vector $k(C_C, C_T)$ falling within the first Brillouin zone. Fig. 8 shows the transformation of the density of states in the upper and lower polaritonic bands caused by the elastic strain.

Let us remind that due to dependence of the period of the "virtual" crystal lattice $d(\{C_T\})$ (and hence of the Brillouin zone) on C_T the domain of definition of the density of states $\rho_\pm(\Omega, \hat{\varepsilon}, C_C, C_T)$ along Ω-axis is also a function of C_T. It is obvious that the function $\rho_\pm(\Omega, \hat{\varepsilon}, C_C, C_T)$ has singularities only at the edges of the frequency interval $\Omega[k_-(C_C, C_T)] < \Omega < \Omega[k_+(C_C, C_T)]$, in a full analogy to the phonon spectra of one-dimensional structures (Ref. [15]). It can be readily seen from Fig. 8 that peculiarities of the spectrum have clear manifestations in the corresponding density of states.

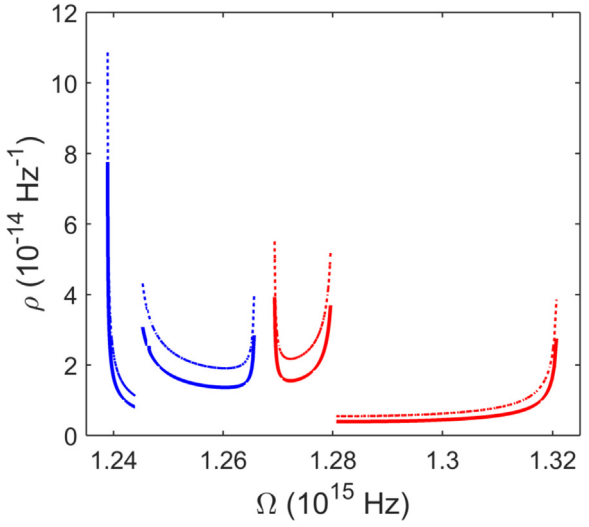

Fig. 8. The strain-induced change of the density of polaritonic states in a one-sublattice quantum-dot-containing chain of unevenly spaced microcavities. Dotted curves correspond to $\varepsilon = 0.4$; solid curves correspond to $\varepsilon = 0$. The values of dot concentrations is taken $C_C = 0.1.C_C = 0.5$

4. Conclusion

The theoretical study of the photonic band structure of binary one-dimensional arrays of tunnel-coupled microcavities shows that subjecting the system to the controllable elastic strain is an effective tool for altering its eigen mode structure and optical properties. This applies both for the cases of microcavity arrays with embedded quantum dots and for quantum-dot-free lattices. The strain and the photonic disorder lead to an increase of the effective mass of the propagating photon modes in the structure and hence to a decrease of their group velocity. This results in formation of slow light modes that can be efficiently controlled by the externally applied strain. These results pave the way to applications of irregular microcavity chains in optical integrated circuits and as classical or quantum optical switches [19]. The considered arrays of coupled optical cavities open promising vistas for fabrication of optical circuits, where the light propagation would be controlled by variable contents of structural “defects” (composition and positions of microcavities) as well as by the alterable magnitude and character of applied strains.

Acknowledgements

A.K. acknowledges the financial support from the Hybrid Polaritonics Programme grant of the EPSRC (EP/M025330/1) and the joint Russian-Greek project supported by Ministry of Education and Science of the Russian Federation (project RFMEFI61617X0085).

References

[1] S.V. Dmitriev, Y.A. Baimova, Effect of elastic deformation on phonon spectrum and characteristics of gap discrete breathers in crystal with NaCl-type structure, Tech. Phys. Lett. 37 (2011) 451.
[2] M.A. Kaliteevskii, Coupled vertical microcavities, Tech. Phys. Lett. 23 (1997) 120.
[3] K.J. Vahala, Optical microcavities, Nature 424 (2003) 839.
[4] A. Askitopoulos, L. Mouchliadis, I. Iorsh, G. Christmann, J.J. Baumberg, M.A. Kaliteevski, Z. Hatzopoulos, P.G. Savvidis, Bragg polaritons: strong coupling and amplification in an unfolded microcavity, Phys. Rev. Lett. 106 (2011) 076401.
[5] D.M. Beggs, M.A. Kaliteevski, S. Brand, R.A. Abram, Optimization of an optical filter with a square-shaped passband based on coupled microcavities, J. Mod. Optic. 51 (2004) 437.
[6] V.V. Rumyantsev, S.A. Fedorov, K.V. Gumennyk, M.V. Proskurenko, Peculiarities of propagation of electromagnetic excitation through a nonideal photonic crystal, Physica B 442 (2014) 57.
[7] V.V. Rumyantsev, S.A. Fedorov, K.V. Gumennyk, M.V. Sychanova, A.V. Kavokin, Exciton-like electromagnetic excitations in non-ideal microcavity supercrystals, Nature Sci. Rep 4 (2014) 6945.
[8] V.V. Rumyantsev, S.A. Fedorov, K.V. Gumennyk, M.V. Sychanova, A.V. Kavokin, Polaritons in a nonideal periodic array of microcavities, Superlattice. Microst. 89 (2016) 409.
[9] E.S. Sedov, A.P. Alodjants, S.M. Arakelian, Y.Y. Lin, R.-K. Lee, Nonlinear properties and stabilities of polaritonic crystals beyond the low-excitation-density limit, Phys. Rev. 84 (2011) 013813.
[10] J.D. Joannopoulos, S.G. Johnson, J.N. Winn, R.D. Meade, Photonic Crystals. Molding the Flow of Light, Princeton University Press, Princeton, 2008.
[11] V.M. Agranovich, Theory of Excitons, Nauka Publishers, Moscow, 1968.
[12] V.V. Rumyantsev, S.A. Fedorov, K.V. Gumennyk, Polaritons in a nonideal array of ultracold quantum dots, Low Temp. Phys. 42 (2016) 347.
[13] Z.S. Yang, N.H. Kwong, R. Binder, A.L. Smirl, Stopping, storing, and releasing light in quantum-well Bragg structures, J. Opt. Soc. Am. B 22 (2005) 2144.
[14] A.V. Turukhin, V.S. Sudarshanam, M.S. Shahriar, J.A. Musser, B.S. Ham, P.R. Hemmer, Observation of ultraslow and stored light pulses in a solid, Phys. Rev. Lett. 88 (2001) 023602–1.
[15] A.M. Kosewicz, Mechanika Fizyczna Nieidealnych Krystalicznych Ciai Staiych, Wyd. Uniwersytetu Wroclawskiego, Wroclaw, 2000.
[16] J.M. Ziman, Models of Disorder: the Theoretical Physics of Homogeneously Disordered Systems, Cambridge University Press, 1979.
[17] V.F. Los, Projection operator method in the theory of disordered systems. I. Spectra of quasiparticles, Theor. Math. Phys. 73 (1987) 1076.
[18] P. Lodahl, S. Mahmoodian, S. Stobbe, Interfacing single photons and single quantum dots with photonic nanostructures, Rev. Mod. Phys. 87 (2015) 347.
[19] P. Tighineanu, A.S. Sørensen, S. Stobbe, P. Lodahl, The mesoscopic nature of quantum dots in photon emission, in: P. Michler (Ed.), Quantum Dots for Quantum Information Technologies. Nano-optics and Nanophotonics, Springer, Cham, 2017, pp. 165–198.